

# Visualizing Spacetime Curvature via Gradient Flows II: An Example of the Construction of a Newtonian analogue

Majd Abdelqader\* and Kayll Lake†

Department of Physics, Queen's University, Kingston, Ontario, Canada, K7L 3N6

(Dated: July 24, 2012)

This is the first in a series of papers in which the gradient flows of fundamental curvature invariants are used to formulate a visualization of curvature. We start with the construction of strict Newtonian analogues (not limits) of solutions to Einstein's equations based on the topology of the associated gradient flows. We do not start with any easy case. Rather, we start with the Curzon - Chazy solution, which, as history shows, is one of the most difficult exact solutions to Einstein's equations to interpret physically. We show that the entire field of the Curzon - Chazy solution, up to a region very "close" to the intrinsic singularity, strictly represents that of a Newtonian ring, as has long been suspected. In this regard, we consider our approach very successful. As regards the local structure of the singularity of the Curzon - Chazy solution within a fully general relativistic analysis, however, whereas we make some advances, the full structure of this singularity remains incompletely resolved.

PACS numbers: 04.20.Cv, 04.20.Ha, 02.70.-c

## I. INTRODUCTION

Perhaps the most familiar example of an exact solution to Einstein's equations, generated by way of a Newtonian "analogue", is the Curzon - Chazy solution wherein the Laplacian for a point mass in a fictitious Euclidean 3-space is used to generate an exact static axially symmetric vacuum solution of Einstein's equations. Unfortunately, the Curzon - Chazy solution bears little resemblance to a point mass. Indeed, its singularity structure appears, at present, to be as complicated as that of the Kerr solution.

In this paper, following the introduction given by one of us [1], we consider the gradient fields of the two non-differential invariants of the Curzon - Chazy solution. These alone reveal previously unknown non-local properties of the solution. Further, following the procedure given in [1] for the construction of strict Newtonian analogues, based on gradient flows, we suggest that a pure Newtonian ring is "almost" a complete analogue of the Curzon - Chazy solution. Whereas our main aim here is the construction of the analogue, we have had to do a fair amount of analysis of the Curzon - Chazy solution itself. Most of this analysis is relegated to Appendices.

## II. THE CURZON-CHAZY METRIC

The line element for a static and axially symmetric spacetime can be written in Weyl's canonical coordinates [2]

$$ds^2 = -e^{2U} dt^2 + e^{-2U} (e^{2\gamma} (d\rho^2 + dz^2) + \rho^2 d\phi^2), \quad (1)$$

where  $U$  and  $\gamma$  are functions of  $\rho$  and  $z$ . It is well known that these coordinates do not behave like typical cylindrical coordinates. Einstein's field equations in vacuum with zero cosmological constant give the following *linear* partial differential equation for  $U$ ,

$$\frac{\partial^2 U}{\partial \rho^2} + \frac{1}{\rho} \frac{\partial U}{\partial \rho} + \frac{\partial^2 U}{\partial z^2} = 0. \quad (2)$$

Equation (2) is Laplace's equation in a Euclidean 3-space in cylindrical polar coordinates. The general solution to (2) can be written out and the associated Einstein equations

$$\frac{\partial \gamma}{\partial \rho} = \rho \left( \left( \frac{\partial U}{\partial \rho} \right)^2 + \left( \frac{\partial U}{\partial z} \right)^2 \right), \quad \frac{\partial \gamma}{\partial z} = 2\rho \frac{\partial U}{\partial \rho} \frac{\partial U}{\partial z} \quad (3)$$

can be considered solved. Since in the weak field we have  $g_{tt} \sim -(1 + 2U)$ , it is tempting to consider a solution-generating procedure wherein one takes a known Newtonian potential  $U$  (in an unphysical Euclidean 3-space), and solves (3) for  $\gamma$ . We then have an exact solution to Einstein's equations. Unfortunately, the resultant Weyl solution bears little similarity to the Newtonian solution and the physical meaning of most Weyl solutions so produced remain unclear. The culprit is the *non-linearity* of Einstein's equations that enters via (3).

The Curzon [3] - Chazy [4] solution (CC hereafter) is one of the simplest special cases of the Weyl metric (1).<sup>1</sup> The potential is taken to be the Newtonian potential of a point mass ( $m$ ) at the center of a fictitious Euclidean 3-space,  $\rho = z = 0$ ,

$$U = -\frac{m}{\sqrt{\rho^2 + z^2}}, \quad m > 0. \quad (4)$$

\* majd@astro.queensu.ca

† lake@astro.queensu.ca

<sup>1</sup> For a review see [5].

With (4) it follows from (3) that

$$\gamma = -\frac{m^2 \rho^2}{2(\rho^2 + z^2)^2}. \quad (5)$$

The resultant metric components are well defined except at  $(\rho, z) = (0, 0)$ . The circumference of a trajectory constant  $t$ ,  $\rho$  and  $z$  is equal to  $2\pi\rho e^{m/\sqrt{\rho^2+z^2}}$ , which behaves like Euclidean cylindrical coordinates for  $\rho/m$  or  $z/m \gg 1$ , but the circumference diverges in the plane

$z = 0$  as  $\rho$  goes to zero. Further, the meaning of  $m$  in the CC solution is no longer obvious. This is discussed below.

Given (4) and (5) it follows that there are two non-vanishing independent polynomial invariants of order  $p = 2$ . For convenience, define

$$r^2 = \rho^2 + z^2. \quad (6)$$

The invariants can be taken to be<sup>2</sup>

$$w1r = 2m^2 \left( e^{\frac{m^2 \rho^2}{r^4}} \right)^2 \frac{(3r^6 - 6mr^5 + 3m^2r^4 + 3m^2\rho^2r^2 - 3\rho^2m^3r + \rho^2m^4)}{r^{12} \left( e^{\frac{m}{r}} \right)^4} \quad (7)$$

and

$$w2r = 3m^3 \left( e^{\frac{m^2 \rho^2}{r^4}} \right)^3 \frac{(m-r)(2r^6 - 4mr^5 + 2m^2r^4 + 3m^2r^2\rho^2 - 3\rho^2m^3r + \rho^2m^4)}{r^{16} \left( e^{\frac{m}{r}} \right)^6}. \quad (8)$$

Clearly, the explicit representation of (7) and (8) is a matter of some choice, but see below. In any event, at first glance, it would appear that  $r = 0$  is singular. However, along  $\rho = 0$ , we note that

$$\chi \equiv -\frac{w2r}{6} \Big|_{\rho=0} = \left( \frac{w1r}{6} \right)^{3/2} \Big|_{\rho=0} = \frac{m^3(z-m)^3}{z^{12} \left( e^{\frac{m}{z}} \right)^6} \quad (9)$$

and, in particular,

$$\lim_{z \rightarrow 0} \chi = 0. \quad (10)$$

Now, whereas  $\chi$  has a local minimum ( $= 0$ ) at  $z = \pm m$ , and a local maximum at  $z = \pm(1 \pm 1/\sqrt{3})m$  (see below), it is clear that there is no scalar polynomial singularity along  $\rho = 0$ . Yet, more generally, except perhaps for selected trajectories,  $w1r$  and  $w2r$  both diverge at  $\rho = z = 0$ . The directional divergence of  $K$  was, as far as we know, first noticed by Gautreau and Anderson [8]. This observation generated much further consideration. In terms of “polar” coordinates  $(r, \theta)$  ( $\rho = r \sin(\theta)$ ,  $z = r \cos(\theta)$ , see below), Stachel [9] showed that the area of surfaces of constant  $t$  and  $r$  decreases with decreasing  $r$  up to a minimum (which can be shown

to be  $r \simeq 0.5389m$ ) and then diverges as  $r \rightarrow 0$ . These surfaces can be shown to be topologically spherical, a point that is important for the construction of the Hawking mass discussed below. Cooperstock and Junevicius [10] showed that even trajectories of the simple form  $z = C\rho^n$ , where  $C$  and  $n$  are positive constants, give  $K$  a rich structure. Further analysis of the geodesics followed in order to explore the singularity and the global structure of the metric [11], [12], [13], [14].<sup>3</sup> The general consensus is that the singularity has a “ring-like”, rather than “point-like”, structure. This is not so simple as it first sounds. The “ring” has finite radius but infinite circumference [12]. Rather remarkably late was the computation of  $w2r$  in [15], a work which gave visual information on the CC metric based on the principal null directions. This procedure gives much less information than the visualization procedure considered here as we explain below. More recently, Taylor [16] has suggested a technique for unraveling directional singularities.<sup>4</sup>

<sup>2</sup> Much of the older literature refers only to the Kretschmann scalar ( $K \equiv \mathcal{R}_{\alpha\beta\mu\nu}\mathcal{R}^{\alpha\beta\mu\nu}$ , where  $\mathcal{R}$  is the Riemann tensor) which, in the modern literature, is not considered a fundamental invariant. See [6] and references therein. In vacua,  $K = 8w1r$  and so nothing is lost by considering  $K$  as opposed to  $w1r$ . However, as explained below,  $w2r$  must also be considered. Note that the notation  $w1r$  and  $w2r$  refers to the real part of the first and second Weyl invariants. Their signs are a matter of convention but we adhere to the conventions in [7].

<sup>3</sup> It is remarkable that the simple coordinates used by Stachel (which we refer to as Stachel, rather than “polar” coordinates) have not been exploited further in the study of the CC metric. This is examined in Appendix A where the relevant results of Cooperstock and Junevicius, and Scott and Szekeres are generalized.

<sup>4</sup> Taylor’s technique is not applicable to the CC solution due to a critical point along  $\rho = 0$  as  $z \rightarrow 0$ . This is explained below.

### III. GRADIENT FIELDS

As in [1] we define the gradient fields<sup>5</sup>

$$k_n^\alpha \equiv \pm \nabla^\alpha \mathcal{I}_n = \pm g^{\alpha\beta} \frac{\partial \mathcal{I}_n}{\partial x^\beta}, \quad (11)$$

where now

$$\mathcal{I}_1 = w1r, \quad \mathcal{I}_2 = w2r. \quad (12)$$

#### A. Stachel Coordinates

The explicit forms for the gradient fields are given in Appendix B in Stachel coordinates. We prefer to draw the flows explicitly in Weyl coordinates as given below, but there is no loss of information in doing this since the inverse transformations,  $r = \sqrt{\rho^2 + z^2}$ ,  $\theta = \arctan(\rho/z)$ , are so simple.<sup>6</sup> A convention we use, based on Stachel coordinates, is that we say that the positive gradient flow is “ingoing” for  $k^r < 0$  and “outgoing” for  $k^r > 0$ .

#### B. Weyl Coordinates

Figures 1 and 2 show the *positive* gradient fields for the CC metric in the first quadrant only, since the metric is axially symmetric, as well as symmetric about the equatorial plane ( $z \rightarrow -z$ ). The first field,  $k_1$ , for the CC metric, has 7 critical points  $(\rho, z)$ :  $(0, 0)$  (along  $\rho = 0, z \rightarrow 0$ ),  $(0, \pm m)$  (stable nodes of index +1 and isotropic critical points [1] with  $w1r = 0$ ),  $(0, \pm m(1 - 1/\sqrt{3}))$  (hyperbolic saddle points of index -1), and  $(0, \pm m(1 + 1/\sqrt{3}))$  (hyperbolic saddle points of index -1). Note that the gradient field is undefined at  $(0, 0)$  (along  $z = 0, \rho \rightarrow 0$ ). The overall index for any hypersurface of constant  $t$  and  $\phi$  is +1 as expected.<sup>7</sup> On the other hand, the second field,  $k_2$  has 8 critical points: the same 7 points as  $k_1$ , except that now  $(0, \pm m)$  is an isotropic critical point with  $w2r = k_2^\alpha = \text{index} = 0$ . In addition we find the critical points  $(\approx 1.11m, 0)$  (stable node of index +1). Again we find that the overall index for any hypersurface of constant  $t$  and  $\phi$  is +1. Note that the field was normalized for visual representation, since it increases exponentially as we approach the origin. This normalization does not

affect the shape of the resulting flow lines. In these plots, the color of the sampled flowlines is used simply to highlight the different regions.

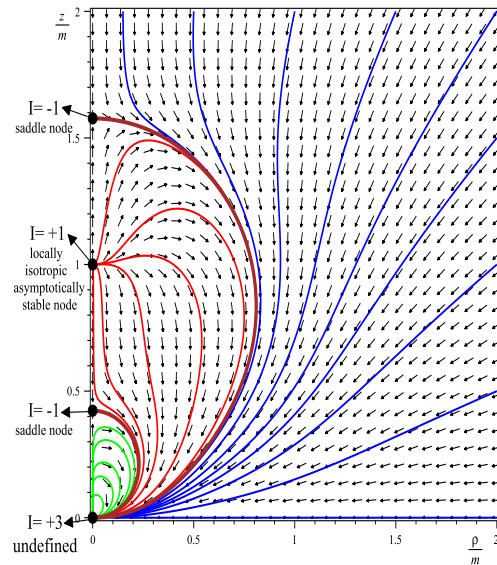


FIG. 1. The positive gradient field  $k_1$  of the Weyl invariant  $w1r$  for the CC metric, presented in Weyl coordinates. The field is normalized for visual representation, and the flowlines are colored to categorize them into distinct groups according to their global behavior (blue, red and green). Critical points are represented by black circles, and critical directions of the fields are shown with their associated indices and are shown and discussed in the text.

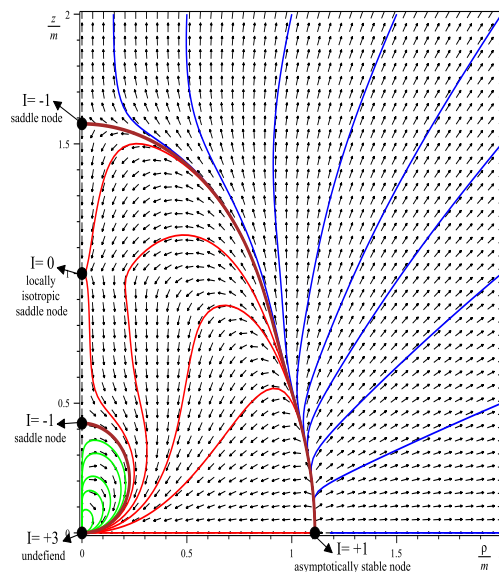


FIG. 2. As in Figure 1 but for  $k_2$ .

As we can see in Figure 1, all of the flowlines of  $k_1$  terminate at the singularity  $(0, 0)$  (approaching it along the

<sup>5</sup> Since we are following the conventions in [7], there is a (physically irrelevant) reversal in the direction of the gradient flow between  $w1r$  and  $w2r$ . We refer to the choice “+” as a positive gradient flow and the choice “-” as a negative gradient flow. We find occasion to use both.

<sup>6</sup> That is, to view the flow in Stachel coordinates simply think of  $r$  as a circle centered on an origin at  $\rho = z = 0$ , and  $\theta$  a straight line through the origin measured from 0 along the vertical to  $\pi/2$  in the equatorial plane.

<sup>7</sup> Of course the indices must be calculated in the full “plane”, for both positive and negative  $z$  and for  $\phi = 0$  and  $\phi = \pi$ .

equatorial plane ( $z = 0, \rho \rightarrow 0$ ). They can be categorized into three distinct regions according to where they originate, separated by two critical directions drawn in brown:

1. Blue region: The flowlines originate from infinity.
2. Red region: The flowlines originate from the critical point  $(0, m)$ , and the critical direction of the gradient field separating the blue and red regions originates from the critical point  $(0, m(1 + 1/\sqrt{3}))$ .
3. Green region: The flowlines originate from the critical point  $(0, 0)$  along the  $z$ -axis. The critical direction separating the red and green regions originates from the critical point  $(0, m(1 - 1/\sqrt{3}))$ .

The picture for the flowlines of  $k_2$  is somewhat different, and is shown in Figure 2. However, we still have three distinct regions separated by two critical directions:

1. Blue region: The flowlines originate from the critical point  $\sim (1.1m, 0)$ , and terminate at infinity.
2. Red region: The flowlines originate from the critical point  $\sim (1.1m, 0)$ , and terminate at  $(0, 0)$ , approaching it along the equatorial plane. The critical direction of the gradient field separating the blue and red regions originates from the critical point  $\sim (1.1m, 0)$ , and terminates at  $(0, m(1 + 1/\sqrt{3}))$ .
3. Green region: The flowlines originate from the critical point  $(0, 0)$  along the  $z$ -axis, and terminate at that point as well approaching it along the equatorial plane. The critical direction separating the red and green regions originates from the critical point  $(0, m(1 - 1/\sqrt{3}))$ , and terminates at  $(0, 0)$ .

### C. Scott - Szekeres Unfolding

The unfolding of  $(\rho, z) = (0, 0)$ , given by Scott and Szekeres in [12] and [13], is reproduced in Appendix C. Spacelike infinity ( $r \rightarrow \infty$ ) is mapped onto  $0 \leq X \leq \pi$  with  $Y = \pi/2$  and  $X = \pi$  with  $0 \leq Y \leq \pi/2$ , the  $z$  axis maps onto  $-\pi/2 < Y < \pi/2$  with  $X = 0$  and the  $\rho$  axis onto  $\pi/2 < X < \pi$  with  $Y = 0$ . Now  $r = 0$  corresponds to  $0 \leq X \leq \pi/2$  with  $Y = -\pi/2$  and  $X = \pi/2$  with  $-\pi/2 \leq Y \leq 0$ . The singularity of the CC metric is represented only by  $X = \pi/2$  with  $Y = 0$ .

The gradient fields of the CC metric, with this unfolding, are shown in Figures 3 and 4. The unfolding of the Weyl coordinate point  $(0, 0)$  is now evident: All of the flowlines for  $k_1$  terminate at the singularity  $(X, Y) = (\pi/2, 0)$ . The flowlines of the green region now originate from a different point, specifically  $(X, Y) = (\pi/2, -\pi/2)$ .

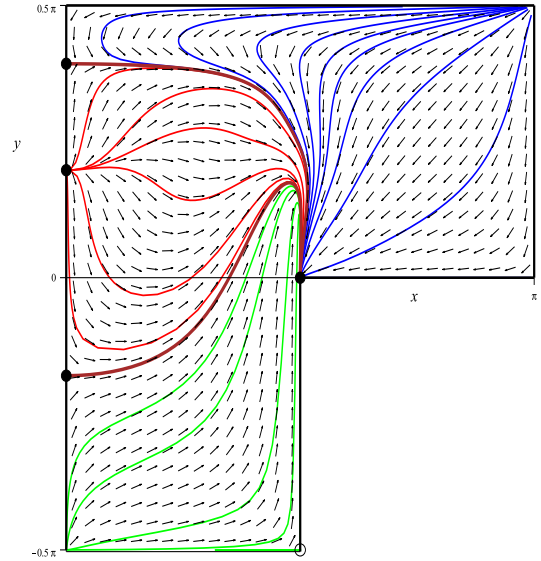


FIG. 3. As in Figure 1 but with the Scott - Szekeres unfolding. All flow lines terminate at the singularity at  $(X, Y) = (\pi/2, 0)$ . All green flow lines originate at  $(X, Y) = (\pi/2, -\pi/2)$  which is the critical point  $(\rho, z) = (0, 0)$  along  $\rho = 0, z \rightarrow 0$ .

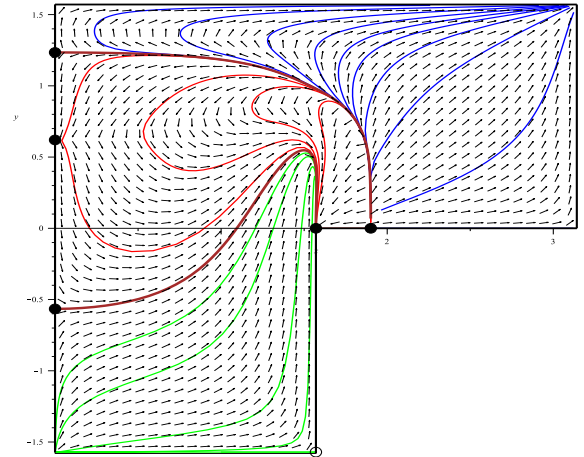


FIG. 4. As in Figure 2 but with the Scott - Szekeres unfolding.

### D. A New Unfolding

Whereas the unfolding of  $(\rho, z) = (0, 0)$  given by Scott and Szekeres accomplishes the task, the rather complicated procedure also modifies the entire spacetime representation. Here we seek a new unfolding of  $(\rho, z) = (0, 0)$  which does not modify the spacetime in the large. It turns out that we need only modify  $\rho$ . On reviewing Appendix A we see that the most important term to consider

is the exponent of  $\sin(\theta)/x$ . We can write

$$\frac{\sin(\theta)}{x} = \frac{\rho m}{r^2}. \quad (13)$$

Now either this exponent diverges or it does not. If it diverges we can compactify this divergence with a tanh function. If it does not diverge we can set the term to zero by multiplying by  $\rho$ . Finally, let us require that the new  $\rho$  and old  $\rho$  approach each other for sufficiently large  $r$ . We arrive at the unfolding

$$\frac{\tilde{\rho}}{m} = \frac{\rho}{m} + \tanh\left(\frac{\rho}{m} e^{\rho m/r^2}\right) \left(1 - \tanh\left(\frac{r}{m}\right)\right). \quad (14)$$

The singularity is at  $(\tilde{\rho}, 0) = (m, 0)$  and the critical point is at  $(\tilde{\rho}, 0) = (0, 0)$ . No flow lines cross the “edge”  $0 < \tilde{\rho} < m$  where  $r = 0$ . Indeed, whereas the trajectories  $\theta = 0$  and  $\theta = \pi$  reach  $\tilde{\rho} = 0$ , all other trajectories of constant  $\theta$  reach  $\tilde{\rho} = m$ . This is shown in figure 5. The gradient fields of the CC metric are shown in Figures 6 and 7 with this new unfolding. It is very important to realize that this unfolding cannot correct all misrepresentations created by the Weyl coordinates. In particular, if the Weyl coordinates do not cover the “edge”, neither does the unfolding.

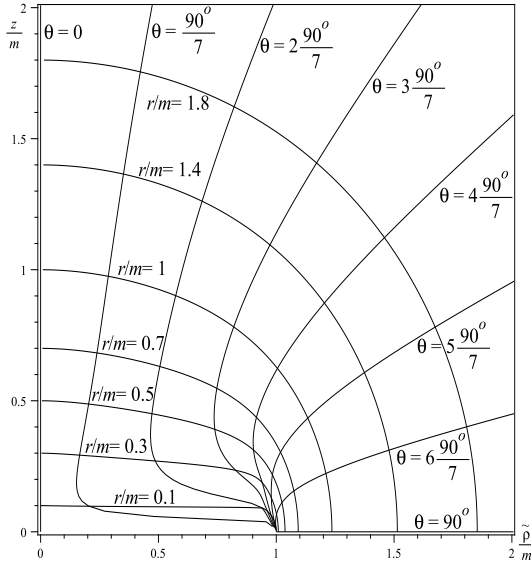


FIG. 5. The  $z/m - \tilde{\rho}/m$  quarter plane. These are *not* oblate spheroidal coordinates. The “edge”  $0 < \tilde{\rho} < m$ , where  $r = 0$ , is not part of the spacetime.

### E. “mass”

Whereas the constant  $m$  has entered the CC solution via the Newtonian potential (4), the meaning of  $m$  within the CC solution is no longer obvious. This is explored in Appendix D where we show that  $m$  is certainly the “mass” at spatial infinity. However, away from spatial

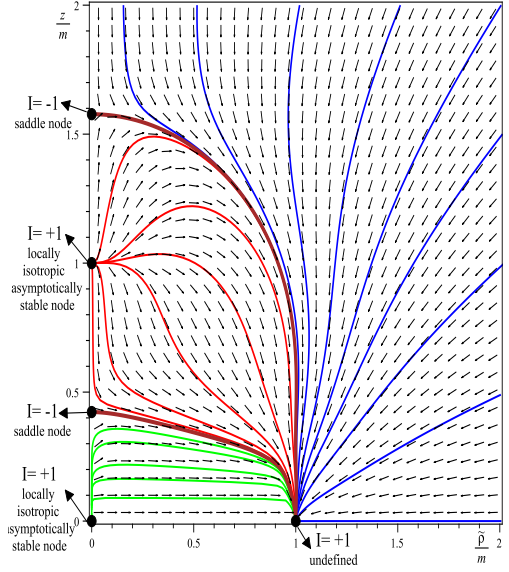


FIG. 6. As in Figure 1 but with the new unfolding.

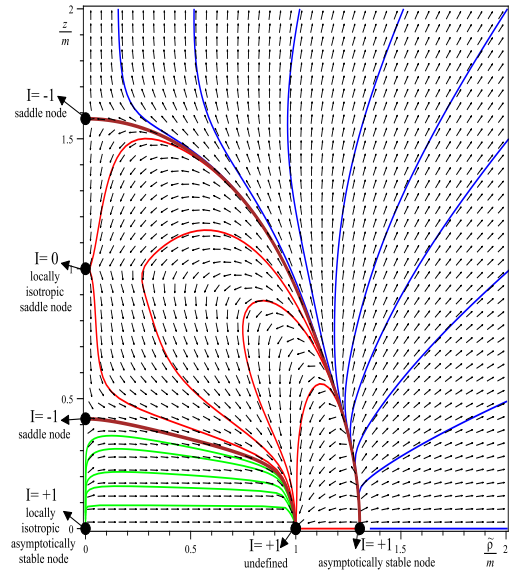


FIG. 7. As in Figure 2 but with the new unfolding.

infinity, looking at quasi local and local constructions, we find that the Hawking mass  $\mathcal{M}_H$  provides no useful information for the CC solution. Rather, it is the classical effective gravitational mass  $\mathcal{M} \equiv \mathcal{R}_{\theta\phi}^{\theta\phi} g_{\theta\theta}^{3/2}/2$  [1] that provides useful information on the CC solution. Whereas this  $\mathcal{M}$  rapidly converges to  $m$  with increasing  $r$ , near  $r = 0$ ,  $\mathcal{M}$  shows considerable structure. Most interesting is the fact that  $\mathcal{M} = 0$  at the (naked) singularity, reminiscent of spherically symmetric naked singularities [20].

#### IV. THE NEWTONIAN ANALOGUE

We finally get to the central consideration of this paper. As explained previously [1], following for example Ellis [21], we construct the Newtonian tidal tensor

$$E_{ab} = \Phi_{,a,b} - \frac{1}{3}\eta_{ab}\square\Phi, \quad (15)$$

and define the associated invariant

$$E_{ab}E^{ab} = \Phi_{,a,b}\Phi^{,a,b} - \frac{1}{3}(\square\Phi)^2. \quad (16)$$

We now construct the gradient field

$$l_1^c \equiv \pm \nabla^c(E_{ab}E^{ab}). \quad (17)$$

We say that  $l_1$  is a Newtonian analogue (in no way any limit) of  $k_1$  if their associated phase portraits are “analogous”, a designation which is explained in detail below. This analogy is strict since, as explained in [1],  $k_1^\alpha = \pm \nabla^\alpha (E_{\beta\gamma}E^{\beta\gamma})$  where  $E_{\beta\gamma}$  is the usual electric component of the Weyl tensor; that is, the general - relativistic tidal tensor in the Ricci - flat case. The generalization of (17) for comparison with  $k_2$  is

$$l_2^d \equiv \pm \nabla^d(E_a^b E_b^c E_c^a). \quad (18)$$

The Newtonian potential for a infinitely thin ring in vacuum with radius  $a$  and mass  $m$  is

$$\Phi_{ring}(\rho, z) = -\frac{\tilde{m}}{2\pi} \int_0^{2\pi} \frac{d\theta}{\sqrt{\tilde{\rho}^2 + \tilde{z}^2 + 1 - 2\tilde{\rho}\cos\theta}}, \quad (19)$$

where  $\tilde{x} \equiv x/a \ \forall x$ . Note that  $m$  only affects the intensity of the gradient field, but does not change the shape of the flowlines or the normalized field when the coordinates are parameterized by the radius. We therefore take  $m = 1$ . Further, since there is no scale set for  $z$ , we take  $\sqrt{2}z$  for visualization. Along the  $z$ -axis, for both  $l_1$  and  $l_2$ , defined by (17) and (18) respectively, we find 5 critical points:  $\sqrt{2}z/a = 0, \pm 1$ , and  $\pm\sqrt{3}$  ( $\sim \pm 1.7$ ). This is to be compared to:  $z/m = 0, \pm 1, \pm(1 - 1/\sqrt{3})$ , and  $\pm(1 + 1/\sqrt{3})$  ( $\sim \pm 1.6$ ) for the CC metric. The Newtonian gradient fields are shown in Figures 8 and 9. In both cases the overall index is +1.

Comparing Figures 6 and 8 we see that the CC metric contains an additional flow (the green flow) not present for a Newtonian ring. Otherwise, the gradient flows are remarkably similar. Comparing Figures 7 and 9 we see that as well as the additional flow in the CC metric, there is also an additional critical point in the equatorial plane not present for a Newtonian ring. Again, otherwise, the gradient flows are remarkably similar.

The green region in the CC solution, which is absent in our Newtonian analogue, indicates that the “source” of the CC metric is not just a Newtonian ring.

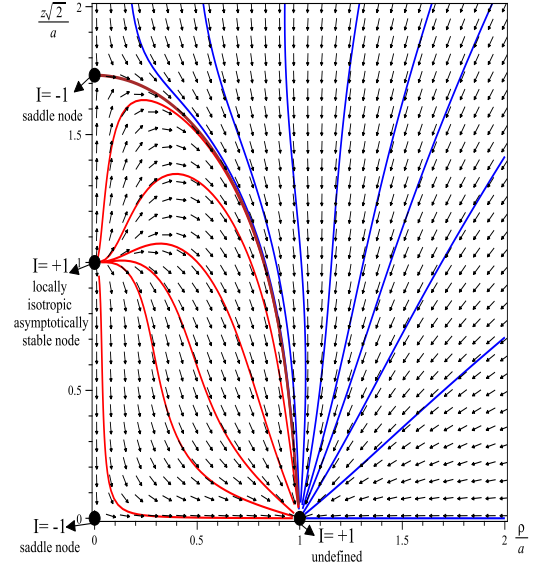


FIG. 8. Gradient field  $l_1$ , defined by (17), for a Newtonian ring in vacuum. Compare Figure 6.

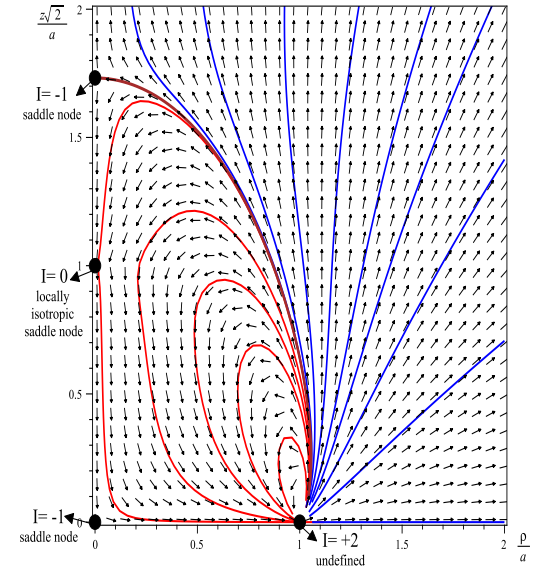


FIG. 9. Gradient field  $l_2$ , defined by (18), for a Newtonian ring in vacuum. Compare Figure 7.

#### V. DISCUSSION AND CONCLUSION

We have demonstrated a new tool designed to visualize spacetime curvature based on the construction of gradient flows of invariants. The emphasis here has been on the construction of strict Newtonian analogues wherein the invariants are the relativistic and Newtonian tidal invariants. The case we have considered, the Curzon - Chazy solution, is by no means an easy case to start out with. Despite this, we have shown that the gradient flows for the tidal invariant in the Curzon - Chazy



solution, and that for an infinitely thin Newtonian ring, are remarkably similar in detail. Only “interior to” and “closely above” the Curzon - Chazy “ring” do the flows differ. This region is absent in the Newtonian case. For completeness we have included all non - differential invariants of the Curzon - Chazy solution and so we have also included a study of the second Weyl invariant and its Newtonian counterpart for an infinitely thin ring. Again we find that the gradient flows are remarkably similar in detail except for the same region close to the Curzon - Chazy ring and the addition of an external, but “close”, critical “ring” of the flow in the equatorial plane not present for the Newtonian ring. Whereas one could,

perhaps, refine the Newtonian counterpart and, perhaps, find sharper agreement, the arguments presented here, we believe, go a long way to clarify the notion that the “source” of the Curzon - Chazy solution is “ring - like” and that the construction of strict Newtonian analogues, correct “in the large”, is possible.

## ACKNOWLEDGMENTS

This work was supported in part by a grant (to KL) from the Natural Sciences and Engineering Research Council of Canada. Portions of this work were made possible by use of *GRTensorII* [22].

- 
- [1] K. Lake, “Visualizing Spacetime Curvature via Gradient Flows I: Introduction” (preprint) (2012).
  - [2] H. Weyl, *Annalen der Physik* **10**, 185 (1919).
  - [3] H. E. J. Curzon, *Proc. London Math. Soc.* **23**, 477 (1925).
  - [4] J. Chazy, *Bull. Soc. Math. France* **52**, 17 (1924).
  - [5] J. Griffiths and J. Podolský, *Exact Space-Times in Einstein’s General Relativity* (Cambridge University Press, Cambridge, 2009).
  - [6] K. Santosuosso, D. Pollney, N. Pelavas, P. Musgrave and K. Lake, *Comput. Phys. Commun.* **115**, 381 (1998) (gr-qc/9809012).
  - [7] J. Carminati and R. G. McLenaghan, *J. Math. Phys.* **32**, 3135 (1991).
  - [8] R. Gautreau and J. L. Anderson, *Physics Letters A* **25**, 291 (1967).
  - [9] J. Stachel, *Physics Letters A* **27**, 60 (1968).
  - [10] F. I. Cooperstock and G. J. Junevicius, *Int. J. Th. Phys.* **9**, 59 (1974).
  - [11] P. Szekeres and F. H. Morgan, *Commun. Math. Phys.* **4**, 313 (1973).
  - [12] S. M. Scott and P. Szekeres, *G. R. G.* **18**, 557 (1986).
  - [13] S. M. Scott and P. Szekeres, *G. R. G.* **18**, 571 (1986).
  - [14] F. de Felice, *G. R. G.* **23**, 135 (1991).
  - [15] R. Arianrhod, S. Fletcher and C. B. G. McIntosh, *Class. Quan. Grav.* **8**, 1519 (1991).
  - [16] J. P. W. Taylor, *Class. Quantum Grav.* **22**, 4961 (2005).
  - [17] E. Poisson, *A Relativist’s Toolkit The Mathematics of Black-Hole Mechanics* (Cambridge University Press, Cambridge, 2004).
  - [18] See, for example, L. B. Szabados, *Living Rev. Relativity*, **12**, (2009), 4 <http://www.livingreviews.org/lrr-2009-4> (Update of lrr-2004-4)
  - [19] Daniel Hansevi, *The Hawking mass for ellipsoidal 2-surfaces in Minkowski and Schwarzschild space-times*, thesis Linköpings Universitet, downloaded from <http://www.mai.liu.se/gober/theses.html>
  - [20] K. Lake, *Phys. Rev. Lett.* **68**, 3129 (1992).
  - [21] See the Editor’s notes *Gen. Rel. Grav.* **41**, 575 (2009) and the article accompanying these notes.
  - [22] This package runs within Maple. The GRTensorII software and documentation is distributed freely from the address <http://grtensor.org>
- 

## Appendix A: Stachel Coordinates

Under the transformations

$$\rho = r \sin(\theta), \quad z = r \cos(\theta) \quad (\text{A1})$$

the CC metric takes the form

$$ds^2 = -e^{-\frac{2m}{r}} dt^2 + e^{\frac{2m}{r}} \left( e^{-\frac{m^2 \sin^2(\theta)}{r^2}} (dr^2 + r^2 d\theta^2) + r^2 \sin^2(\theta) d\phi^2 \right). \quad (\text{A2})$$

Either from (A2), or from CC metric and (A1), we obtain

$$w1 \equiv (w1r)m^4 = 2e^{2t1} \frac{(3t2 + \sin(\theta)^2 t3)}{x^{10}} \quad (\text{A3})$$

and

$$w2 \equiv (w2r)m^6 = -3e^{3t1} \frac{(x-1)(2t2 + \sin(\theta)^2 t3)}{x^{14}} \quad (\text{A4})$$

where

$$x \equiv r/m, \quad (\text{A5})$$

$$t1 \equiv \frac{\sin(\theta)^2 - 2x}{x^2}, \quad (\text{A6})$$

$$t2 \equiv x^2(x-1)^2, \quad (\text{A7})$$

and

$$t3 \equiv 3x^2 - 3x + 1. \quad (\text{A8})$$

Now let us take

$$\sin(\theta) \equiv a(x), \quad (\text{A9})$$

where  $0 \leq a \leq 1$ , in order to define trajectories  $\theta(x)$ . We are interested in limits as  $x \rightarrow 0$ . First let us assume  $a \in C^2$ .

*i)*  $a(0) = a_o \neq 0$

We find

$$w1 \sim 2e^{2\frac{a_o^2}{x^2}} \frac{a_o^2}{x^{10}} \rightarrow \infty, \quad (\text{A10})$$

and

$$w2 \sim -3e^{3\frac{a_o^2}{x^2}} \frac{a_o^2}{x^{14}} \rightarrow -\infty. \quad (\text{A11})$$

*ii)*  $a(0) = 0$

We find

$$w1 \sim \frac{6}{e^{\frac{4}{x}} x^8} \rightarrow 0, \quad (\text{A12})$$

and

$$w2 \sim -\frac{6}{e^{\frac{6}{x}} x^{12}} \rightarrow 0. \quad (\text{A13})$$

Historically,  $a \in C^0$  have played a role. Following [10], in the notation of [12], consider the trajectories

$$\frac{z}{m} = b\left(\frac{1}{2}\right)^{\frac{1}{3}} \left(\frac{\rho}{m}\right)^n, \quad (b, n > 0), \quad (\text{A14})$$

that is,

$$x \cos(\theta) = b\left(\frac{1}{2}\right)^{\frac{1}{3}} (x \sin(\theta))^n. \quad (\text{A15})$$

Now if  $a(0) = 0$ , we can use the small angle formula to obtain

$$a = \frac{x^{\frac{1-n}{n}}}{B^{\frac{1}{n}}}, \quad B \equiv b\left(\frac{1}{2}\right)^{\frac{1}{3}}. \quad (\text{A16})$$

Of particular interest is the case  $n = 2/3$  for which

$$a = \left(\frac{2x}{b^3}\right)^{\frac{1}{2}}. \quad (\text{A17})$$



For the convergence of  $w1$  and  $w2$  we must have

$$\frac{a^2 - 2x}{x^2} < 0, \quad (\text{A18})$$

that is,  $b > 1$  for the case (A17). This is the correction in [12] to an error in [10]. Further details concerning the very particular choice (A14) can be found in [12]. Here we simply note that  $a \in C^1$  requires  $n < 1/2$  and  $a \in C^2$  requires  $n < 1/3$  for this particular choice. In [12], Scott and Szekeres go on to argue (on page 562) that they found a trajectory along which the Kretschmann scalar goes to a finite non - zero constant as  $r \rightarrow 0$ . We have examined this claim in detail and find the claim to be false. Along the suggested trajectory we find that the Kretschmann scalar goes to zero.<sup>8</sup> Our understanding is that only two limits are possible within known coordinates: zero and  $\pm$  infinity.

Now for the metric (A2),  $\xi^\alpha = \delta_t^\alpha$  is a Killing vector. As a result, for all geodesics with tangents  $u^\alpha$  we have a constant of the motion  $\xi^\alpha u_\alpha \equiv -\gamma$ . As a result, for all geodesics we have

$$\frac{dt}{d\lambda} = \pm \gamma e^{\frac{2}{x}} \quad (\text{A19})$$

where  $\lambda$  is an affine parameter. This shows the inadequacy of the coordinate  $t$  as  $x \rightarrow 0$ .

## Appendix B: Gradient Fields in Stachel Coordinates

The contravariant gradient flow associated with the invariant  $w1r$  is given by

$$m^5 k_1^r = \pm 2e^{3t1} \frac{\sin(\theta)^2(4\sin(\theta)^2 t3 + t4) + 6t5}{x^{13}} \quad (\text{B1})$$

and

$$m^6 k_1^\theta = \mp 4e^{3t1} \frac{\sin(\theta) \cos(\theta)(2\sin(\theta)^2 t3 + t6)}{x^{14}} \quad (\text{B2})$$

where

$$t4 \equiv x(36x^3 - 63x^2 + 34x - 4), \quad (\text{B3})$$

$$t5 \equiv x^3(3x^2 - 6x + 2)(x - 1), \quad (\text{B4})$$

and

$$t6 \equiv x^2(9x^2 - 15x + 7). \quad (\text{B5})$$

The contravariant gradient flow associated with the invariant  $w2r$  is given by

$$m^7 k_2^r = \mp 3e^{4t1} \frac{6(x-1)t5 + \sin(\theta)^2(6\sin(\theta)^2(x-1)t3 + xt7)}{x^{17}} \quad (\text{B6})$$

where

$$t7 \equiv 45x^4 - 126x^3 + 124x^2 - 50x + 6, \quad (\text{B7})$$

and

$$m^8 k_2^\theta = \pm 6e^{4t1} \frac{\sin(\theta) \cos(\theta)(x-1)(3\sin(\theta)^2 t3 + t6)}{x^{18}}. \quad (\text{B8})$$

Note that the upper sign corresponds to a negative gradient flow in all cases above.

---

<sup>8</sup> This is rather unfortunate in the sense that had the claim been correct, a further unfolding of the singularity would be absolutely

necessary for a complete understanding of the singularity.

### Appendix C: Scott - Szekeres Unfolding

The unfolding of  $(\rho, z) = (0, 0)$  given by Scott and Szekeres in [12] and [13], obtained by trial and error, is

$$X = \arctan((\rho/m) e^{m/z}) + \arctan((\rho/m) e^{(-\sqrt{2}m/\rho)^{2/3}}) \quad (C1)$$

and

$$Y = \arctan \left( 3 \frac{z}{m} - \frac{(z/m)^2 e^{m/r - m^2 \rho^2 / 2r^4}}{((r/m)^8 + 1 + \frac{1}{3}(\rho/m)^2 (r/m)^{-4})^{1/4}} \right) \quad (C2)$$

in Weyl coordinates. In Stachel coordinates we find

$$X = \arctan(x \sin(\theta) e^{1/x \cos(\theta)}) + \arctan(x \sin(\theta) e^{(-\sqrt{2}/x \sin(\theta))^{2/3}}) \quad (C3)$$

and

$$Y = \arctan \left( 3x \cos(\theta) - \frac{x^2 \cos(\theta)^2 e^{-t^{1/2}}}{(x^8 + 1 + \sin(\theta)^2 / 3x^2)^{1/4}} \right). \quad (C4)$$

### Appendix D: “mass”

We are interested to see how the constant  $m$  in the CC solution is related to “mass”. First, let us rewrite (A2) via Taylor series about  $1/r = 0$  with explicit terms to order  $1/r$ . We have

$$ds^2 = -\left(1 - \frac{2m}{r}\right)dt^2 + \left(1 + \frac{2m}{r}\right)(dr^2 + r^2 d\Omega_2^2) \quad (D1)$$

where  $d\Omega_2^2$  is the metric of a unit 2-sphere ( $d\theta^2 + \sin^2(\theta)d\phi^2$ ). To this order in  $r$  we find that the Einstein tensor for (D1) vanishes. Due to the spherical symmetry of (D1) we can consider the mass defined by  $\mathcal{M} \equiv \mathcal{R}_{\theta}{}^{\theta}{}_{\phi}{}^{\phi} g_{\theta\theta}^{3/2} / 2$  [1]. To order  $1/r$  we find

$$\mathcal{M} = m - \frac{3m^2}{2} \left( \frac{1}{r} \right). \quad (D2)$$

As a result, at spatial infinity,  $m$  is the “mass”. We need not consider the ADM mass, the Komar integrals nor the Bondi -Sachs mass [17]. Rather, we are interested in exploring the meaning of  $m$  away from spatial infinity. We are, therefore, interested in local and quasi-local quantities.

Let us look at the Hawking mass [18], which can be defined by

$$\mathcal{M}_H = \left( \frac{A(\mathcal{S})}{16\pi} \right)^{1/2} \left( 1 - \frac{1}{2\pi} \oint_{\mathcal{S}} \rho \mu d\mathcal{S} \right) \quad (D3)$$

where  $\mathcal{S}$  is a spacelike topological two-sphere,  $A(\mathcal{S})$  is the associated area and here  $\rho$  and  $\mu$  are the Newman - Penrose spin coefficients. As mentioned above, Stachel [9] showed that for  $\mathcal{S}$  defined by surfaces of constant  $t$  and  $r$  in (A2),  $A$  decreases with decreasing  $r$  up to a minimum (which we find to be  $r \simeq 0.5389m$ ) and then diverges as  $r \rightarrow 0$ . To ensure that  $\mathcal{S}$  is a topological two - sphere we use the standard Gauss - Bonnet theorem

$$\frac{1}{2} \int \int_{\mathcal{S}} \mathcal{R} \sqrt{g} dx^a dx^b = 2\pi \chi(\mathcal{S}) \quad (D4)$$

where  $x^a$  are the coordinates on  $\mathcal{S}$ ,  $g$  is the determinant of the metric on  $\mathcal{S}$ ,  $\mathcal{R}$  is the Ricci scalar on  $\mathcal{S}$ , and  $\chi(\mathcal{S})$  is the Euler characteristic of  $\mathcal{S}$ . Again taking  $\mathcal{S}$  to be defined by surfaces of constant  $t$  and  $r$  in (A2) we find

$$\chi(\mathcal{S}) = 2, \quad (D5)$$

and so we are indeed considering topological two - spheres. Constructing a complex null tetrad in the usual way, we find that for (A2)

$$-\rho\mu = -\frac{1}{8} \frac{e^{\frac{m^2 \sin(\theta)^2}{r^2}} (-2mr + 2r^2 + m^2 \sin(\theta)^2)^2}{e^{(\frac{m}{r})^2} r^6} \quad (D6)$$

and so we find

$$\frac{\mathcal{M}_H}{m} = -1/32 \sqrt{2} e^y \sqrt{\int_0^\pi \frac{\sin(\theta)}{\sqrt{e^{(\sin(\theta))^2 y^2}}} d\theta} \left( -8 + \int_0^\pi e^{-(2-y+(\cos(\theta))^2 y)} y \left( 2y - 2 - y^2 + (\cos(\theta))^2 y^2 \right)^2 d\theta \right) y^{-1} \quad (\text{D7})$$

where  $y \equiv m/r = 1/x$ . Expanding about  $y = 0$  we find that

$$\frac{\mathcal{M}_H}{m} = \frac{3\pi}{4} + \frac{1}{2} + \left( \frac{1}{2} - \frac{\pi}{4} \right) \frac{r}{m} + \mathcal{O}\left(\frac{m}{r}\right) \quad (\text{D8})$$

and so, for large  $r$ ,  $\mathcal{M}_H$  is not a reasonable measure of “mass” for the CC solution. Examining (D7) in more detail we find that  $\mathcal{M}_H = 0$  for  $r/m \sim 8.86$ ,  $\mathcal{M}_H$  reaches a maximum  $\mathcal{M}_H/m \sim 1.25$  at  $r/m \sim 2.2$  and  $\mathcal{M}_H \rightarrow -\infty$  as  $r \rightarrow 0$ . We have to conclude that  $\mathcal{M}_H$  is nowhere a measure of “mass” for the CC solution. In this regard, one is reminded of the result of Hansevi [19] who showed that the Hawking mass can be negative even for convex two - surfaces in Minkowski spacetime.

Returning to  $\mathcal{M} \equiv \mathcal{R}_{\theta\phi}^{\theta\phi} g_{\theta\theta}^{3/2}/2$ , whereas this quantity is usually restricted to strict spherical symmetry, it is well defined for (A2). Indeed, a straightforward calculation gives

$$\frac{\mathcal{M}}{m} = e^{-\frac{t1}{2}} \left( 1 + \frac{t1}{2} \right), \quad (\text{D9})$$

where  $t1$  is given by (A6). Continuing with (A9) we find

$$\lim_{x \rightarrow 0} \left( \frac{\mathcal{M}}{m} \right) \rightarrow 0, \quad (\text{D10})$$

for  $a(0) = a_o \neq 0$  and

$$\lim_{x \rightarrow 0} \left( \frac{\mathcal{M}}{m} \right) \rightarrow -\infty, \quad (\text{D11})$$

for  $a(0) = a_o = 0$ . In strict spherical symmetry, it is known that naked singularities are massless ( $\mathcal{M} = 0$ ) [20]. The result (D10) suggests that this might hold away from spherical symmetry. It should be noted that  $\frac{\mathcal{M}}{m}$  converges very rapidly to 1 for all  $\theta$  with increasing  $x$ . We conclude that  $\mathcal{M}$ , if not the “mass”, at least summarizes some important properties of the CC solution.

---